Developmental Cell, Vol. 2, 567–578, May, 2002, Copyright ©2002 by Cell Press

Zinc Ions and Cation Diffusion Facilitator Proteins Regulate Ras-Mediated Signaling

Janelle J. Bruinsma,[1] Tanawat Jirakulaporn,[2,3] Anthony J. Muslin,[2,3] and Kerry Kornfeld[1,4]
[1] Department of Molecular Biology and Pharmacology
[2] Department of Medicine
[3] Department of Cell Biology and Physiology
Washington University School of Medicine
St. Louis, Missouri 63110

Summary

C. elegans cdf-1 **was identified in a genetic screen for regulators of Ras-mediated signaling. CDF-1 is a cation diffusion facilitator protein that is structurally and functionally similar to vertebrate ZnT-1. These proteins have an evolutionarily conserved function as positive regulators of the Ras pathway, and the Ras pathway has an evolutionarily conserved ability to respond to CDF proteins. CDF proteins regulate Ras-mediated signaling by promoting Zn^{2+} efflux and reducing the concentration of cytosolic Zn^{2+}, and cytosolic Zn^{2+} negatively regulates Ras-mediated signaling. Physiological concentrations of Zn^{2+} cause a significant inhibition of Ras-mediated signaling. These findings suggest that Zn^{2+} negatively regulates a conserved element of the signaling pathway and that Zn^{2+} regulation is important for maintaining the inactive state of the Ras pathway.**

Introduction

Ras is a pivotal signaling protein that regulates many cellular processes, and mutations that activate Ras are a common cause of human tumors (Barbacid, 1987). A major pathway that regulates Ras involves a receptor tyrosine kinase (RTK), such as the epidermal growth factor receptor (Cantley et al., 1991; Dickson and Hafen, 1994; Marshall, 1994). Ligand binding stimulates receptor autophosphorylation and creates docking sites for a complex of a phosphotyrosine binding protein, such as GRB2/SEM-5, and a Ras guanine nucleotide exchange factor (RasGEF). RasGEF catalyzes GDP release, resulting in GTP binding and Ras activation. Activated Ras can bind and activate the serine/threonine kinase Raf. Activated Raf phosphorylates and thereby activates a mitogen-activated protein (MAP) kinase kinase, named MEK, which in turn phosphorylates and thereby activates extracellular signal-regulated kinase (ERK) MAP kinase. ERK phosphorylates a variety of target proteins, including transcription factors, and these modifications elicit an appropriate cellular response.

In the nematode *C. elegans*, Ras-mediated signaling controls multiple developmental events; the most extensively analyzed is the induction of the hermaphrodite vulva (Horvitz and Sternberg, 1991). The vulva is a specialized epidermal structure used for egg laying and sperm entry that is formed by the descendants of three ectodermal blast cells, P5.p, P6.p, and P7.p. In wild-type hermaphrodites, the anchor cell of the somatic gonad signals to P6.p using a LIN-3 epidermal growth factor-like ligand. LIN-3 binds to the LET-23 RTK, and this leads to the activation of the SEM-5 adaptor protein, the LET-341 RasGEF, LET-60 Ras, LIN-45 Raf, MEK-2, and MPK-1 ERK MAP kinase (reviewed by Kornfeld [1997]; Greenwald [1997]; Sternberg and Han [1998]). In response to activation of the Ras pathway, P6.p adopts the 1° vulval cell fate (eight descendants). P6.p then signals to P5.p and P7.p through the LIN-12 Notch receptor, causing these cells to adopt the 2° vulval cell fate (seven descendants). While P3.p, P4.p, and P8.p are capable of adopting vulval fates, they appear to receive neither of these signals and thus adopt the nonvulval 3° cell fate (two descendants). In hermaphrodites with a loss-of-function mutation in any of the core signaling genes, P5.p, P6.p, and P7.p adopt nonvulval 3° fates, resulting in a worm with a vulvaless (Vul) phenotype. By contrast, in hermaphrodites with a gain-of-function mutation that constitutively activates the *let-60 ras* gene, P3.p, P4.p, and P8.p often inappropriately adopt vulval fates; the resulting ectopic tissue forms a series of ventral protrusions, called the multivulva (Muv) phenotype. We conducted a genetic screen for mutations that suppress the Muv phenotype caused by activated LET-60 Ras. Alleles of core signaling proteins, such as LIN-45 Raf, MEK-2, and MPK-1 and alleles of modulators, such as KSR-1, were identified (Lackner et al., 1994; Kornfeld et al., 1995a, 1995b). The mutation *n2527* was also identified in this screen, and we previously described a method for high-resolution mapping relative to single-nucleotide polymorphisms that was used to map the *n2527* mutation (Jakubowski and Kornfeld, 1999). The *n2527* mutation affects a previously uncharacterized gene that we named *cdf-1* because it encodes a predicted protein that is similar to members of the cation diffusion facilitator (CDF) family.

The CDF protein family is ancient and ubiquitous (Paulsen and Saier, 1997). Genetic analysis of CDF proteins indicates that they regulate the transport of heavy metal ions. Overexpression of yeast ZRC1 or COT1 confers resistance to toxic levels of zinc or cobalt, respectively, while deletion mutants are hypersensitive to metal toxicity (Kamizono et al., 1989; Conklin et al., 1992). COT1 is localized to mitochondria, suggesting that COT1 transports cobalt from the cytoplasm to the mitochondrial lumen. Overexpression of mammalian ZnT-1 or ZnT-2 rescues a cell line that is hypersensitive to Zn^{2+} toxicity (Palmiter and Findley, 1995; Palmiter et al., 1996). ZnT-1 is localized to the plasma membrane and increases the rate of Zn^{2+} efflux from cells, indicating that ZnT-1 transports Zn^{2+} from the cytoplasm to the extracellular space (Palmiter and Findley, 1995). In these cases, CDF proteins appear to confer increased tolerance to heavy metal ion toxicity by reducing the cytosolic concentration of heavy metal ions. CDF proteins contain six predicted transmembrane domains; the

[4] Correspondence: kornfeld@pcg.wustl.edu

amino and carboxyl termini are predicted to reside intracellularly. The cytoplasmic loop between transmembrane domains IV and V contains clusters of histidine residues that have been hypothesized to bind metals (Paulsen and Saier, 1997). The mechanism of action of CDF proteins has not been established; it is possible that they directly transport metals across cellular membranes, or they may facilitate the function of another transporter (McMahon and Cousins, 1998). CDF proteins have not been reported to regulate Ras-mediated signaling.

Here we describe a molecular and genetic characterization of *C. elegans cdf-1*. *cdf-1* loss-of-function mutations reduced Ras-mediated signaling, suggesting that *cdf-1* positively regulates Ras signaling. Vertebrate ZnT-1 can positively regulate Ras signaling in *C. elegans* and *Xenopus laevis* oocytes, indicating that the ability of CDF proteins to promote Ras signaling and the ability of the signaling pathway to respond to CDF proteins have been conserved during evolution. *cdf-1(lf)* mutants are hypersensitive to Zn^{2+} toxicity, indicating that CDF-1 regulates Zn^{2+} concentrations. These observations suggest that Zn^{2+} negatively regulates the Ras signaling pathway. Consistent with this model, we demonstrated that *C. elegans* exposed to supplemental zinc displayed impaired Ras signaling and that injection of Zn^{2+} into *Xenopus* oocytes reduced Ras signaling. Physiological levels of Zn^{2+} appear to inhibit Ras signaling, since overexpression of CDF proteins enhanced Ras-mediated signaling in *C. elegans* and *Xenopus.* These findings suggest that a conserved protein in the signaling cascade is negatively regulated by Zn^{2+} and that Zn^{2+} inhibition plays an important role in maintaining the inactive state of the Ras pathway.

Results

cdf-1 Encodes a Member of the Cation Diffusion Facilitator Family

The *n2527* mutation was isolated based on its suppression of the *let-60(n1046gf)* Muv phenotype. *n2527* defined a complementation group that was mapped to a 9.6 kb interval of chromosome *X* that contains the open reading frame C15B12.7 (Jakubowski and Kornfeld, 1999). This gene assignment was confirmed by demonstrating that C15B12.7 contains a nonsense mutation in the *n2527* strain and that a fragment of genomic DNA containing C15B12.7 could rescue the *n2527* mutant phenotype in transgenic animals. We named this gene *cdf-1*.

To elucidate the structure of the mRNA and predicted protein products of *cdf-1*, we analyzed *cdf-1* cDNAs. We isolated three cDNAs by hybridization of C15B12.7 sequences to cDNA libraries and obtained one cDNA from the *C. elegans* EST project (Kohara, 1996). By comparing the sequences of these cDNAs with the previously determined sequence of genomic DNA, we determined that *cdf-1* contains seven exons that span 4.2 kb (Figure 1A). The longest cDNA was 1.8 kb, and it contained an SL1 *trans*-spliced leader sequence that identifies the 5′ end of exon 1. Another cDNA terminated with a series of A residues not present in the genomic DNA that identify the poly(A) addition site at the 3′ end of exon 7. Exon junctions were identical in the four cDNAs. The longest predicted open reading frame encodes a 519-amino acid protein. These results indicate that full-length *cdf-1* mRNA contains an SL1 *trans*-spliced leader sequence, 75 nucleotides of 5′ untranslated region, 1557 nucleotides of coding region, 357 nucleotides of 3′ untranslated region, and a poly(A) tail.

The predicted CDF-1 protein shares significant similarity with members of the cation diffusion facilitator family (Figure 1B). CDF-1 displays highest conservation within the six predicted transmembrane domains and has a cluster of histidine residues between membrane spanning domains IV and V. Overall, CDF-1 is about 30% identical to the most similar vertebrate and yeast proteins, murine ZnT-1 and *S. cerevisiae* COT1, respectively. The *cdf-1(n2527)* mutation causes a premature stop at codon 157 that results in a protein that lacks three membrane-spanning domains, suggesting that *cdf-1(n2527)* is a strong loss-of-function mutation (Figure 1B). This is consistent with our genetic analysis, since *cdf-1(n2527)* homozygous and hemizygous mutants display similar suppression of the *let-60(gf)* Muv phenotype (Jakubowski and Kornfeld, 1999). We obtained a second allele, *cdf-1(ok192)*, from the *C. elegans* gene knockout consortium. DNA sequencing showed that the *cdf-1(ok192)* mutation is a deletion that eliminates DNA encoding residues 35–152 and results in a protein that lacks three transmembrane domains (Figure 1B).

CDF-1 Positively Regulates Ras-Mediated Signaling

cdf-1(n2527) is a very effective suppressor of the Muv phenotype caused by the *let-60(n1046gf G13E)* mutation, reducing the penetrance from 84% to 2% Muv. This Muv phenotype was also strongly suppressed in *cdf-1(ok192)* and *cdf-1(n2527)/cdf-1(ok192)* mutants (Table 1, rows 1–4). To investigate the cellular events that account for the suppression of Muv phenotype, we used Nomarski optics to examine the fates of P3.p, P4.p, and P8.p. In *let-60(n1046gf)* single mutants, 37% of these cells adopted complete or partial vulval cell fates ($n = 36$). By contrast, in *let-60(n1046gf); cdf-1(n2527)* double mutants, P3.p, P4.p, and P8.p always adopted an uninduced 3° cell fate ($n = 36$). Thus, the suppression of Muv phenotype caused by *cdf-1* mutations is due to a transformation of vulval to nonvulval cell fates in P3.p, P4.p, and P8.p, and *cdf-1* appears to regulate the initial step in Pn.p cell fate determination.

In an otherwise wild-type genetic background, the *cdf-1(n2527)* and *cdf-1(ok192)* mutations did not cause gross defects in vulval development or egg laying. To determine whether *cdf-1* mutations cause subtle defects in vulval development, we examined the descendants of P5.p–P7.p in L4 hermaphrodites. Only 33% of *cdf-1(ok192)* mutants and 50% of *cdf-1(n2527)* mutants displayed the normal number of 22 descendants (Table 2, rows 1–3). The average number of descendants of P5.p–P7.p in these mutants was 21, and some mutants displayed as few as 18. This small difference is likely to be significant, since it was caused by both alleles and wild-type animals invariably have 22 descendants. Although the precise lineage defects in the mutants were not determined, the typical case of 21 descendants is likely to result from a failure of one of the cells in the 1° or 2° lineage to undergo the final cell division. A loss of

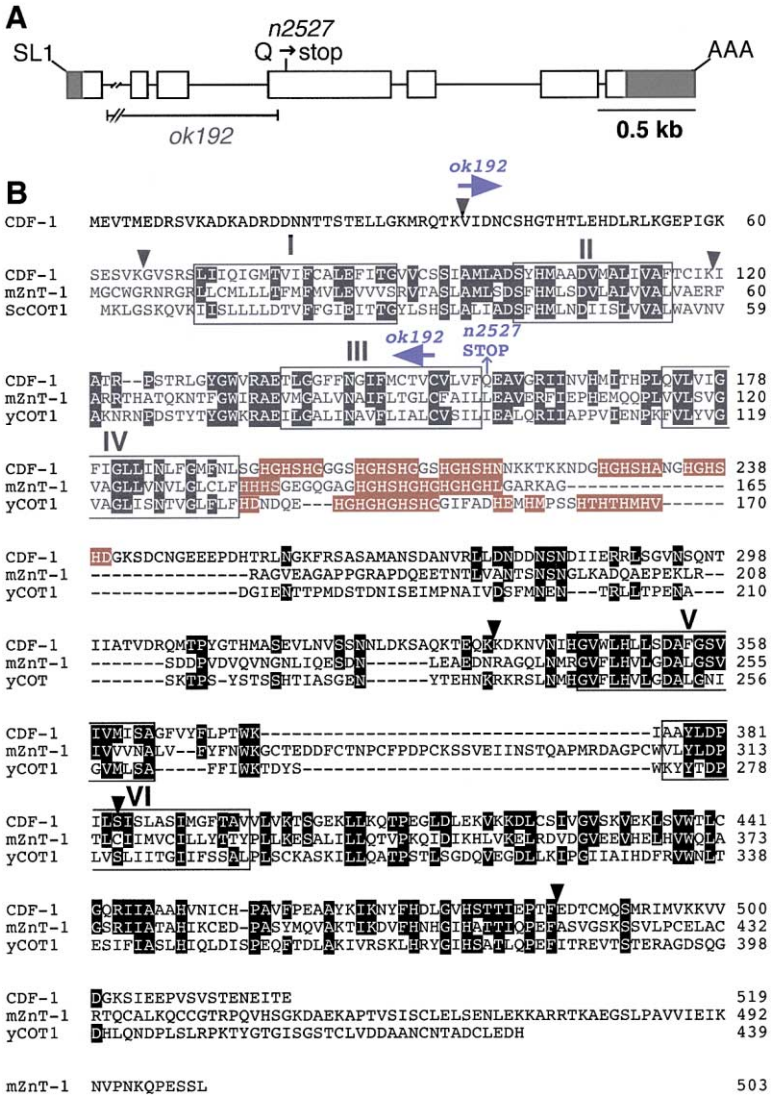

Figure 1. *cdf-1* Encodes a Member of the Cation Diffusion Facilitator Protein Family

(A) *cdf-1* gene structure. Exons, boxes; introns, lines; untranslated regions, gray. The position of the *cdf-1(n2527)* nonsense mutation is shown above; the region of genomic DNA deleted by the *cdf-1(ok192)* mutation (2.025 kb) is indicated below. Diagonal lines indicate the addition sites of the SL1 *trans*-spliced leader and poly(A) tract.

(B) The predicted CDF-1 protein is aligned with the predicted mouse ZnT-1 (Palmiter and Findley, 1995) and *S. cerevisiae* COT1 (Conklin et al., 1992) proteins. Predicted membrane-spanning domains are boxed and labeled with Roman numerals. Clusters of histidine residues following transmembrane domain IV are in red. In CDF-1, this region contains five motifs with the consensus sequence HGHSHX, where X is G, N, A, or D. The positions of introns in *cdf-1* are indicated by arrowheads. The blue arrows indicate the boundaries of the coding region removed by the *cdf-1(ok192)* deletion mutation and the position of the *cdf-1(n2527)* nonsense mutation.

cdf-1 activity caused a more striking defect in a sensitized genetic background. *lin-1* encodes an ETS domain-containing transcription factor that inhibits Pn.p cells from adopting vulval fates; the *lin-1(n1761gf)* mutation results in constitutive LIN-1 activity and a weak Vul phenotype (Jacobs et al., 1998). The *lin-1(n1761gf); cdf-1(n2527)* double mutants had an intermediate strength Vul phenotype; the majority of these animals were egg-laying defective, and P5.p–P7.p generated an average of 16 descendants (Table 2, row 5). These results demonstrate that *cdf-1* is necessary for P5.p–P7.p to execute normal vulval fates and indicate that *cdf-1* positively regulates Ras-mediated signaling during vulval induction.

Many components of the Ras signaling pathway have the property that a loss of activity diminishes signaling and a gain of activity enhances signaling. To determine whether CDF-1 has similar properties, we overexpressed wild-type CDF-1 in worms. Transgenic worms containing extrachromosomal arrays comprised of multiple copies of *cdf-1* genomic DNA were generated by germline transformation. These arrays can rescue the *cdf-1(n2527)* suppression of *let-60(gf)* Muv phenotype (Jakubowski and Kornfeld, 1999). In an otherwise wild-type background, overexpression of CDF-1 did not cause an obvious phenotype. In a sensitized genetic background, overexpression of CDF-1 enhanced the Muv phenotype caused by two different gain-of-function alleles of *let-60 ras* that are partially penetrant and temperature sensitive (Table 1, rows 16–19). These results indicate that CDF-1 activity is sufficient to enhance Ras-mediated signaling.

To explore the relationship between *cdf-1* and other genes that mediate Ras signaling during development, we analyzed double mutants containing a *cdf-1(lf)* mutation and a mutation that causes a Muv phenotype (see Experimental Procedures for a description of these mutations). *cdf-1(n2527)* suppressed the Muv phenotype caused by two different alleles of *let-60 ras, let-60 (n1046gf G13E)* and *let-60(ga89gf L19F)*, demonstrating that the interaction between *cdf-1* and *let-60 ras* is not allele specific (Table 1, rows 1–6). *cdf-1(n2527)* partially suppressed the Muv phenotypes caused by a gain-of-function mutation in the *let-23* RTK and a loss-of-function mutation in *lin-15* (Table 1, rows 7–10). *lin-15* encodes two novel proteins that negatively regulate vulval

Table 1. Interactions between *cdf-1* and Vulval Determination Genes

Genotype	Percentage Muv	N[a]
let-60(n1046gf)	84	518
let-60(n1046gf); cdf-1(n2527)	2	580
let-60(n1046gf); cdf-1(ok192)[b]	7	572
let-60(n1046gf); cdf-1(n2527)/cdf-1(ok192)[c]	5	484
let-60(ga89gf)[d]	17	276
let-60(ga89gf); cdf-1(n2527)[d]	1	630
let-23(sa62gf)[e]	82	390
let-23(sa62gf); cdf-1(n2527)[e]	18	680
lin-15(n765)[f]	55	357
cdf-1(n2527) lin-15(n765)[f]	7	432
lin-1(e1275)[f]	62	371
lin-1(e1275); cdf-1(n2527)[f]	58	270
lin-12(n137gf)	98	284
lin-12(n137gf); cdf-1(n2527)[g]	98	314
amEx28[h]	0	249
let-60(n1046gf)[i]	29	392
let-60(n1046gf); amEx28[h,i]	95	342
let-60(ga89gf)[j]	12	490
let-60(ga89gf); amEx28[h,j]	66	336

We scored all of the adult hermaphrodites on several Petri dishes for the Muv phenotype, one or more ventral protrusions displaced from the position of the vulva. Unless otherwise noted, animals were raised at 20°C.

[a] N, number of hermaphrodites examined.

[b] Complete genotype: *let-60(n1046); lon-2 cdf-1(ok192)*.

[c] Complete genotype: *let-60(n1046); cdf-1(n2527) unc-18/lon-2 cdf-1(ok192)*.

[d] Animals were raised at 25°C.

[e] Complete genotype: *let-23(sa62) unc-4; lon-2 cdf-1(n2527)*. Animals were raised at 15°C.

[f] Animals were raised at 17.5°C.

[g] Complete genotype: *lin-12(n137); lon-2 cdf-1(n2527)*.

[h] *amEx28* is an extrachromosomal array comprised of multiple copies of pJJ4 (genomic *cdf-1*) and the transformation marker pRF4. Multiple, independently derived, transgenic lines were generated in each case; these data are from one representative line of each genotype.

[i] Animals were raised at 15°C.

[j] Animals were raised at 22.5°C.

induction and appear to function upstream of *let-23* by genetic criteria (Clark et al., 1994; Huang et al., 1994). *cdf-1(n2527)* did not suppress the Muv phenotypes caused by a loss-of-function mutation in the *lin-1* ETS transcription factor or a gain-of-function mutation in *lin-12*, a Notch homolog that signals P5.p and P7.p to adopt 2° vulval cell fates (Table 1, rows 11–14). The ability of cells to adopt vulval fates in *lin-1* and *lin-12* mutants indicates that the loss of *cdf-1* activity does not prevent the execution of vulval fates and supports the hypothesis that *cdf-1* specifically influences Ras-mediated signaling.

CDF-1 Expression Pattern and Site of Action

To determine the expression pattern of CDF-1, we generated a plasmid that encodes full-length CDF-1 with the C terminus fused to green fluorescent protein (GFP) expressed by the endogenous *cdf-1* promoter (Figure 2A). Transgenic worms were generated that had the genotype *let-60(gf); cdf-1(n2527)* and contained an extrachromosomal array of this plasmid and a transformation marker. These animals displayed full rescue of the *cdf-1* suppression of *let-60(gf)* Muv phenotype, indicating that the expression pattern of the fusion protein is likely to be similar to that of endogenous CDF-1 (Figure 2A). GFP was highly expressed in the vulval muscles and the intestinal cells; the expression was most intense at the junctions between the pharynx and intestine and the intestine and the rectum (Figures 2B–2E and data not shown). GFP was expressed moderately in the descendants of P5.p, P6.p, and P7.p. In addition, GFP was expressed in ectopic pseudovulvae (Figures 2B and 2C). It is noteworthy that the formation of these ectopic pseudovulvae requires the function of the CDF-1::GFP fusion protein, as the *let-60(gf)* Muv phenotype is effectively suppressed by the *cdf-1(lf)* mutation. A significant GFP signal was not detected in other cells. The CDF-1::GFP fusion protein is concentrated at the edge of the intestinal cells and the descendants of the Pn.p cells, indicating that it is localized to the plasma membrane.

To determine the site of action of CDF-1 during vulval development, we used heterologous promoters to express CDF-1 in the Pn.p cells or the intestinal cells. A *cdf-1* cDNA was used to minimize the possibility of including promoter elements from the *cdf-1* locus, and a translational fusion to GFP was included to provide introns that are necessary for processing transcripts in *C. elegans* (Mello et al., 1991). As a positive control, the *cdf-1* cDNA was expressed under the control of the endogenous *cdf-1* promoter. The resulting extrachromosomal array rescued the *cdf-1* mutant phenotype, albeit somewhat less effectively that the genomic *cdf-1* construct (Figure 2A). We did not detect GFP in these transgenic animals, indicating that the level of expression is significantly lower than in transgenic animals

Table 2. *cdf-1* Mutations Cause a Weak Vulvaless Phenotype

Genotype	P5.p–P7.p Descendants[a]	Percentage with 22 Descendants[b]	N[c]
wild type	22 (22)	100	12
cdf-1(n2527)	21 (18–22)	50	12
cdf-1(ok192)	21 (19–22)	33	12
lin-1(n1761gf)[d]	21 (19–22)	46	13
lin-1(n1761gf); cdf-1(n2527)[d]	16 (8–21)	0	14

[a] P5.p–P7.p descendants, the number of nuclei that appeared to be descendants of P5.p, P6.p, and P7.p based on appearance and position in L4 hermaphrodites at the "Christmas tree" stage of vulval development. The number is an average followed by the smallest and largest values observed.

[b] Percentage with 22 descendants, the fraction of hermaphrodites with 22 descendants of P5.p–P7.p.

[c] N, number of L4 hermaphrodites examined.

[d] These strains also contained *dpy-20(e1282)*.

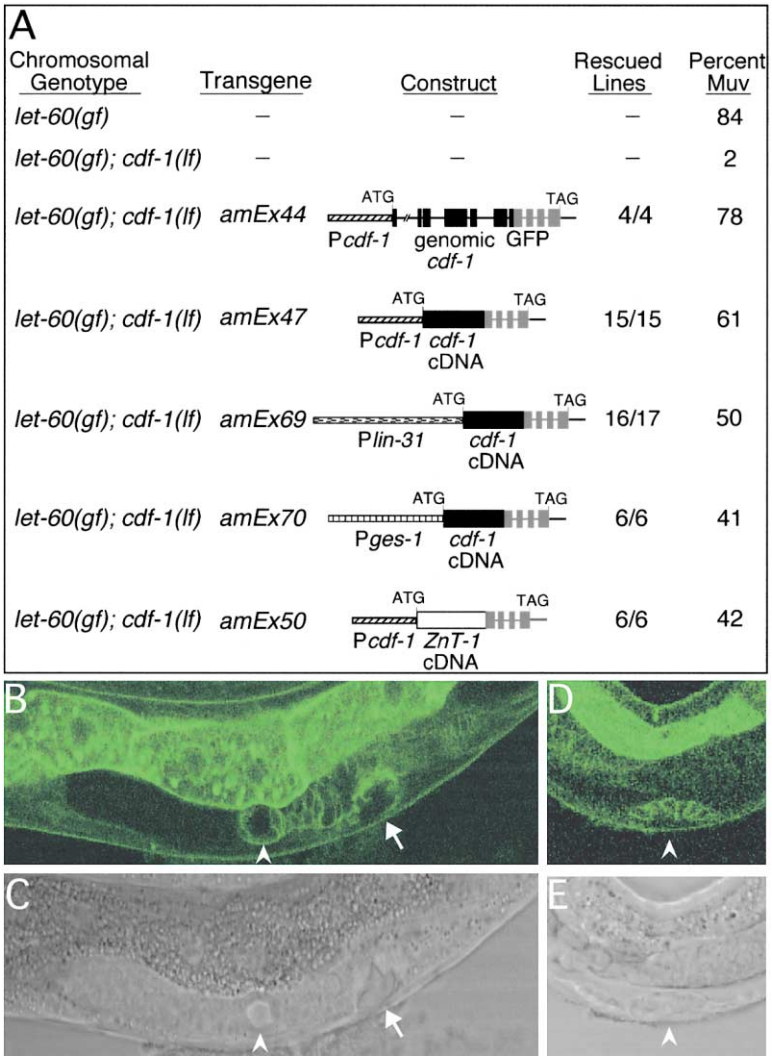

Figure 2. CDF-1 Expression Pattern, Site of Action, and Functional Similarity to Vertebrate ZnT-1

(A) The complete genotype of each strain is indicated by mutations (chromosomal genotype) and extrachromosomal arrays (transgene). The portion of the array that encodes a CDF protein is illustrated (construct). Promoters consisted of 1.6 kb of DNA upstream of the *cdf-1* initiation codon (P*cdf-1*, hatched box), the promoter of the *lin-31* gene (P*lin-31*, stippled box) or the promoter of the *ges-1* gene (P*ges-1*, vertical-striped box). *cdf-1*, black; introns, thin lines; exons, boxes; rat ZnT-1, white; GFP, gray. The start (ATG) and stop (TAG) codons are indicated. *amEx44* contains pJJ16 and pRF4, a transformation marker (see Experimental Procedures). *amEx47* contains pJJ17 and pRF4, *amEx50* contains pJJ23 and pRF4, *amEx69* contains pJJ25 and pRF4, and *amEx70* contains pJJ24 and pRF4. Rescued lines indicate the number of independently derived transgenic strains that displayed rescue of the *n2527* suppression of *let-60(n1046gf)* Muv phenotype and the total number of strains analyzed. We defined rescue as greater than 30% Muv for transgenic animals; nontransgenic siblings were about 2% Muv. The percentage of Muv shown is data from one representative line.

(B–E) Early L4 stage *let-60(gf); cdf-1(lf); amEx44* hermaphrodites seen in a ventral/lateral view (B and C) or a lateral view (D and E). Confocal microscopy was used to visualize GFP fluorescence (B and D) or cell nuclei using Nomarski optics (C and E). Arrowheads indicate the normal vulval invagination that displays significant GFP expression. Arrows indicate an ectopic invagination that displays significant GFP expression. The intestine is the intensely fluorescent tubular organ positioned dorsal to the vulva. The intense, punctate staining in the cytoplasm of intestinal cells is caused by autofluorescent granules and is observed in control worms that do not express GFP. GFP was highly expressed at the periphery of the intestinal cells and the descendants of Pn.p cells that adopted vulval cell fates.

containing the genomic *cdf-1* construct. These differences might be caused by reduced transcription or RNA processing. To investigate CDF-1 function in the Pn.p cells, we used the promoter of the *lin-31* gene that is specifically expressed in the Pn.p cells (Tan et al., 1998). Transgenic worms containing this construct displayed substantial rescue of the suppression of *let-60(gf)* Muv phenotype (Figure 2A). A typical strain displayed about 50% Muv animals, and several strains displayed complete rescue of the phenotype. We did not detect a GFP signal in these animals, indicating that the fusion protein is not highly expressed. These findings indicate that CDF-1 expression in the Pn.p cells is sufficient to rescue the mutant phenotype and that CDF-1 functions cell autonomously in the Pn.p cells.

To investigate CDF-1 function in the intestinal cells, we fused the CDF-1::GFP translational fusion to the promoter of the *ges-1* gene that is expressed specifically in intestinal cells (Aamodt et al., 1991). Transgenic worms containing this construct as an extrachromosomal array displayed partial rescue of the suppression of *let-60(gf)* Muv phenotype (Figure 2A). Thus, CDF-1 expression in the intestinal cells can partially rescue the defects in vulval development, indicating that CDF-1 can function cell nonautonomously in addition to functioning cell autonomously.

Vertebrate ZnT-1 Regulates Ras-Mediated Signaling in Vertebrates and *C. elegans*

CDF proteins have not been reported to be involved in Ras-mediated signaling. To test whether this is a conserved function of CDF proteins, we investigated whether a vertebrate CDF protein could regulate Ras signaling in *C. elegans* and *Xenopus.* We chose rat ZnT-1 because this is the vertebrate protein that is most similar to CDF-1. To express ZnT-1 in *C. elegans*, we generated a plasmid containing the *cdf-1* promoter upstream of the rat *ZnT-1* cDNA fused to GFP. Transgenic animals

containing the plasmid as an extrachromosomal array displayed partial rescue, increasing the penetrance of the Muv phenotype from 2% to 42% (Figure 2A). The finding that rat ZnT-1 rescued the *cdf-1* mutant phenotype somewhat less effectively than the *C. elegans* CDF-1 might indicate differences in expression or protein function. The observation that rat ZnT-1 can substitute for *C. elegans* CDF-1 demonstrates that ZnT-1 is a functional homolog of CDF-1 and that CDF proteins have a conserved function as mediators of Ras signaling.

To investigate whether CDF proteins can regulate the vertebrate Ras-signaling pathway, we analyzed the effect of overexpression of CDF proteins on Ras signaling in *Xenopus* oocytes. Progesterone is the physiological stimulator of meiotic maturation of *Xenopus* oocytes; however, insulin can stimulate maturation by signaling through a Ras/Raf/MEK/ERK pathway that causes oocytes to undergo germinal vesicle breakdown (GVBD) (Korn et al., 1987; Xing et al., 1997). Injection of RNA encoding rat ZnT-1 or *C. elegans* CDF-1 did not induce GVBD compared to control injection of water in oocytes that were otherwise not stimulated (data not shown). However, in combination with the stimulator insulin, injection of rat *ZnT-1* RNA or *C. elegans cdf-1* RNA increased the percent of oocytes that displayed GVBD at multiple time points (Figures 3A and 3C). Injection of rat *ZnT-1* RNA or *C. elegans cdf-1* RNA also stimulated GVBD in oocytes that were costimulated by injection of *Ha-Ras*^{V12} RNA, albeit to a lesser extent (data not shown). Thus, CDF protein activity is sufficient to stimulate Ras signaling in *Xenopus.* To determine the position of CDF protein action in the signaling pathway, we examined phosphorylation of ERK by MEK using a phospho-specific antibody. Injection of rat *ZnT-1* RNA or *C. elegans cdf-1* RNA in combination with the stimulator insulin increased phosphorylation of ERK (Figures 3B and 3D). Thus, CDF proteins are likely to function upstream of ERK MAP kinase in the signaling pathway. These results indicate that CDF proteins have a conserved function as mediators of Ras signaling and that the vertebrate and *C. elegans* Ras pathways have a conserved ability to respond to CDF activity.

CDF-1 Affects Zinc Metabolism in *C. elegans*

CDF proteins in yeast and mammalian cells function to reduce the cytosolic concentration of heavy metal ions by promoting ion transport into vesicles or the extracellular space. To test the hypothesis that *C. elegans* CDF-1 has a similar function and to identify the heavy metal ion(s) that it regulates, we exposed worms to heavy metal ions and monitored their response. If CDF-1 function reduces the cytosolic concentration of a heavy metal ion, *cdf-1(lf)* mutants might be hypersensitive to that ion, and overexpression of CDF-1 might confer resistance to high ion concentrations. Nematodes were raised on a solid agar surface and fed a bacterial lawn. To expose worms to additional metal ions, we supplemented standard nematode growth media (NGM) agar with zinc, cobalt, copper, or cadmium. NGM agar is not defined but presumably contains all of the essential metal ions.

Wild-type worms developed normally on NGM agar plates with 0.25, 0.5, 1, and 2 mM supplemental Zn^{2+}. Two millimolar was the limit of Zn^{2+} solubility under these conditions. Because supplemental Zn^{2+} did not cause significant defects in wild-type animals, it was not possible to use this system to determine whether CDF-1 overexpression causes resistance to elevated Zn^{2+}. In contrast to wild-type animals, *cdf-1(ok192)* and *cdf-1(n2527)* mutants raised on NGM agar plates with supplemental Zn^{2+} displayed dose-dependent developmental defects (Figure 4A). Four days after egg laying, fewer than 50% of *cdf-1(ok192)* and no *cdf-1(n2527)* animals had matured to the adult stage when raised on plates supplemented with 2 mM Zn^{2+}. Many mutants died during larval development, whereas some were developmentally retarded but eventually matured to form adults. Among the mutants that matured to adulthood, 18% of *cdf-1(ok192)* and 12% of *cdf-1(n2527)* mutants were sterile; this phenotype was not displayed by the wild-type animals. These phenotypes appear to be caused by a loss of CDF-1 activity, since overexpression of wild-type CDF-1 fully rescued the *cdf-1(n2527)* hypersensitivity to Zn^{2+} (Figure 4A). Furthermore, overexpression of rat ZnT-1 also fully rescued the *cdf-1 (n2527)* hypersensitivity to Zn^{2+}, demonstrating that CDF-1 and rat ZnT-1 are functionally interchangeable mediators of zinc metabolism. *cdf-1(ok192)* and *cdf-1 (n2527)* mutants displayed a low penetrance of developmental defects under standard growth conditions. These defects may be caused by sensitivity to the basal concentration of Zn^{2+} in NGM media. The finding that *cdf-1(lf)* mutants are hypersensitive to Zn^{2+} suggests that CDF-1 is involved in zinc metabolism and functions to decrease the concentration of cytosolic Zn^{2+}.

Wild-type animals displayed dose-dependent developmental defects in the presence of supplemental cobalt. *cdf-1(lf)* mutants displayed defects that were similar to wild-type animals; they did not display hypersensitivity (Figure 4B). Wild-type animals raised on plates supplemented with 100 μM copper or 25 μM cadmium displayed a low penetrance of developmental defects. *cdf-1(lf)* mutants displayed similar defects to those in wild-type animals under these conditions, indicating that *cdf-1(lf)* does not cause hypersensitivity to copper or cadmium (data not shown). The finding that *cdf-1(lf)* mutants are hypersensitive to zinc but not cobalt, copper, or cadmium indicates that CDF-1 is specifically involved in regulating zinc metabolism. Furthermore, the observation that *cdf-1(lf)* mutants tolerate toxic concentrations of cobalt, copper, or cadmium as well as wild-type worms indicates that the *cdf-1* mutations do not cause a general defect in stress resistance.

Zinc Ions Inhibit Ras-Mediated Signaling

The observations described above suggest the hypothesis that CDF proteins positively regulate Ras signaling by reducing the concentration of cytosolic Zn^{2+} and that Zn^{2+} inhibits Ras signaling. This hypothesis predicts that increasing the cytosolic Zn^{2+} concentration will inhibit Ras signaling, whereas decreasing the cytosolic Zn^{2+} concentration will enhance Ras signaling. To test this prediction, we directly manipulated Zn^{2+} concentrations

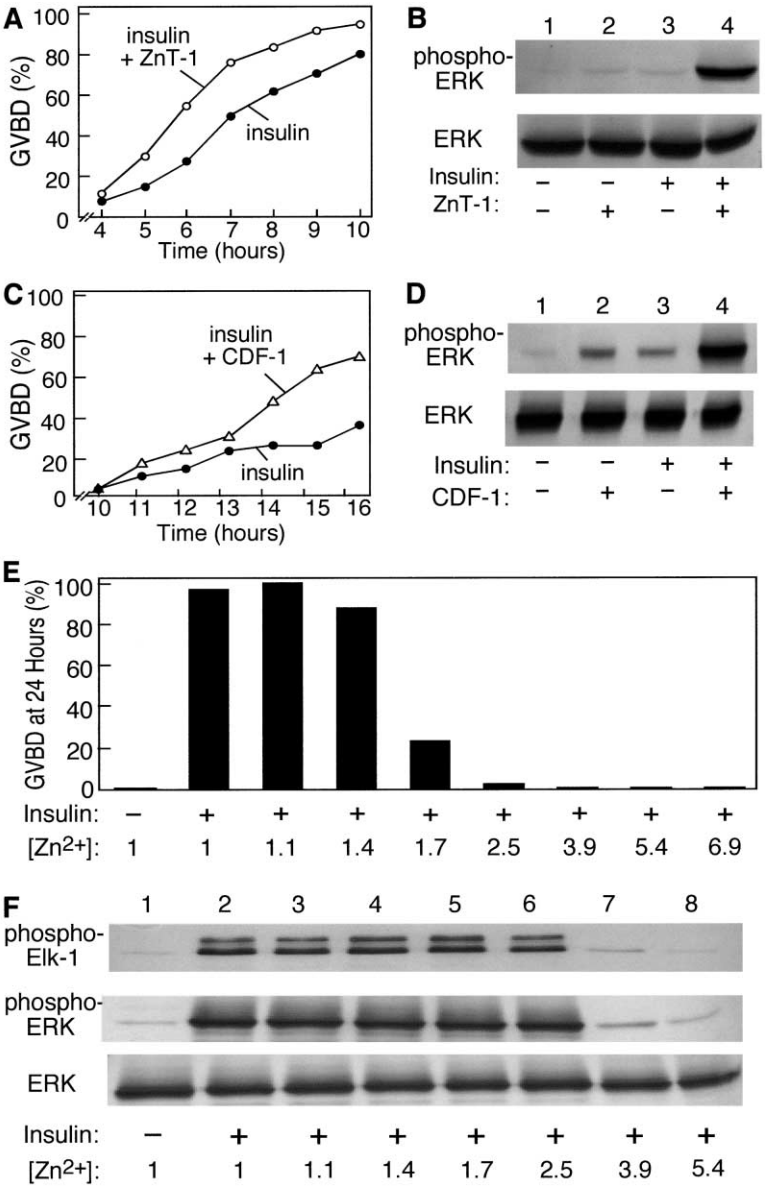

Figure 3. CDF Proteins Positively Regulate Ras Signaling, and Zn^{2+} Negatively Regulates Ras Signaling in *Xenopus* Oocytes

(A) Immature *Xenopus* oocytes were microinjected with water as a control or rat *ZnT-1* RNA and then treated with insulin. For each experiment, 30–60 oocytes were examined at various time points after injection for GVBD. In general, oocytes that were not stimulated did not undergo GVBD, whereas 100% of oocytes treated with insulin eventually displayed GVBD (data not shown). However, the timing of GVBD varied with each batch of oocytes; in panels (A) and (C), the most informative times are shown. A chi-square analysis with continuity correction showed that *ZnT-1* RNA significantly accelerated GVBD at 7 hr ($p = 0.003$).

(B) Oocytes were injected with water (lanes 1 and 3) or RNA encoding rat ZnT-1 (lanes 2 and 4). After 12–24 hr, the injected oocytes were stimulated with insulin (lanes 3 and 4) or left unstimulated (lanes 1 and 2). After 12 hr, oocytes were pooled and examined by Western blot analysis using an antibody that specifically reacts with ERK phosphorylated at the TXY motif recognized by MEK (upper panel) and an antibody that reacts against phosphorylated and nonphosphorylated ERK as a loading control (lower panel).

(C and D) Panels (C) and (D) were essentially as described for panels (A) and (B), respectively, except that *C. elegans cdf-1* RNA was used instead of *ZnT-1* RNA. A chi-square analysis with continuity correction showed that *cdf-1* RNA significantly accelerated GVBD at 15 hr ($p = 0.01$).

(E) The endogenous concentration of Zn^{2+} in oocytes is 1 mM (Nomizu et al., 1993). Oocytes were injected with a solution of $ZnSO_4$ to achieve a calculated total concentration indicated in millimolar (see Experimental Procedures for a description of the calculations); no Zn^{2+} was injected in columns 1 and 2. After 12 hr, the injected oocytes were stimulated with insulin (+) or left unstimulated (−). GVBD was scored after 24 hr of insulin treatment.

(F) Oocytes were treated as in panel (E), pooled after 24 hr, and analyzed by Western blot analysis as in panel (B). In addition, anti-phospho-ERK immunoprecipitates were assayed for ERK kinase activity using recombinant Elk-1 as a substrate (phospho-Elk-1). The experiments shown in panels (A)–(F) were repeated 2–4 times, and similar results were obtained.

and monitored the Ras pathway. Wild-type animals raised on NGM agar supplemented with 2 mM zinc developed a functional vulva, indicating that supplemental zinc does not dramatically impair Ras signaling. To determine whether Zn^{2+} can modulate Ras signaling, we examined the effect of supplemental Zn^{2+} on vulval development using sensitized genetic backgrounds. Supplemental zinc (250 μM) reduced the penetrance of the Muv phenotypes caused by *let-60(n1046gf G13E)* and *let-60(ga89gf L19F)* from 78% to 18% and from 20% to 4%, respectively (Table 3, rows 1–5). Otherwise, these mutants appeared to develop normally. These results suggest that the supplemental Zn^{2+} interferes with Ras-mediated signaling. Supplemental Zn^{2+} also suppressed the Muv phenotypes caused by a *lin-15(lf)* mutation or a *let-23(gf)* mutation (Table 3, rows 6–9). Supplemental Zn^{2+} did not suppress the Muv phenotype caused by a *lin-1(lf)* or a *lin-12(gf)* mutation (Table 3, rows 10–13). These results demonstrate that Zn^{2+} does not generally interfere with the ability of Pn.p cells to adopt a vulval fate. There is a striking similarity between the pattern of Muv suppression caused by supplemental Zn^{2+} and a *cdf-1(lf)* mutation (compare Tables 1 and 3); this finding indicates that Zn^{2+} and *cdf-1* act at the same step in the Ras pathway and supports the hypothesis that *cdf-1* modulates Ras signaling by affecting the cytosolic concentration of Zn^{2+}.

The observation that supplemental Zn^{2+} suppressed the *let-60(gf)* Muv phenotype made it possible to use this assay to investigate the effect of CDF-1 overexpression. Overexpression of CDF-1 reversed the suppression of Muv caused by 250 μM supplemental Zn^{2+} (Table 3,

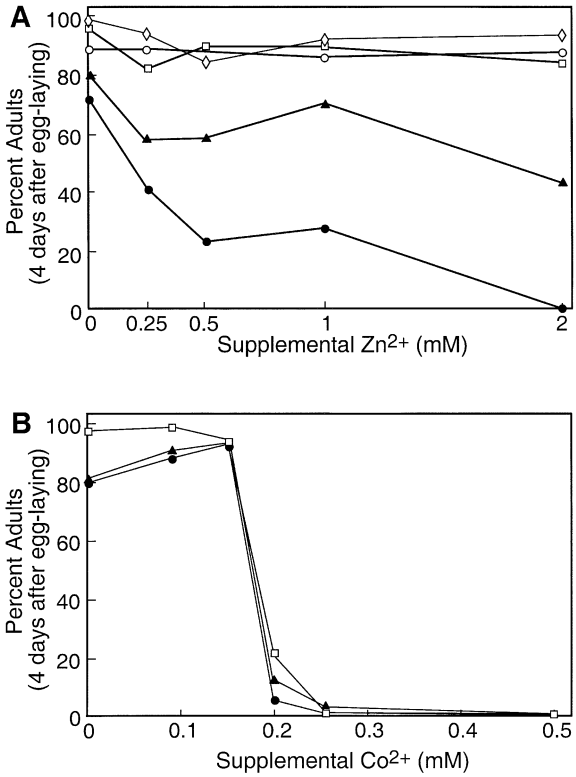

Figure 4. *cdf-1* Mutants Are Hypersensitive to Zinc

Eggs were placed on NGM agar plates with supplemental $ZnSO_4$ (A) or $CoCl_2$ (B), and development was monitored daily; the percentage of animals that reached adulthood within four days is shown. Each data point represents at least 100 eggs. Wild-type, open squares; *cdf-1(ok192)*, closed triangles; *cdf-1(n2527)*, closed circles; *cdf-1(n2527); amEx33*, open circles; *cdf-1(n2527); amEx50*, open diamonds. *amEx33* is an extrachromosomal array containing multiple copies of pJJ4, which contains genomic *cdf-1* and the transformation marker pRF4. *amEx50* is an extrachromosomal array containing multiple copies of pJJ23, which contains rat *ZnT-1* cDNA and the transformation marker pRF4. The Pearson's chi-square test revealed that the difference between the development of N2 and both *cdf-1(n2527)* and *cdf-1(ok192)* was highly significant ($p < 0.001$) at all concentrations of supplemental zinc.

row 3). These data support the hypothesis that *cdf-1* functions to reduce the concentration of cytosolic Zn^{2+}.

To test the hypothesis that Zn^{2+} negatively regulates Ras signaling in vertebrates, we increased the concentration of cytosolic Zn^{2+} in *Xenopus* oocytes and analyzed Ras signaling. *Xenopus* oocytes have a volume of about 1 μl and a Zn^{2+} concentration of about 1 mM (Nomizu et al., 1993). By microinjecting $ZnSO_4$ into *Xenopus* oocytes, we directly manipulated the cytosolic concentration of Zn^{2+} by a defined amount. Injection of Zn^{2+} to yield a total oocyte concentration of 1.1 mM or 1.4 mM did not significantly affect GVBD stimulated by insulin (Figure 3E). Injection of Zn^{2+} to yield a total oocyte concentration of 1.7 mM reduced GVBD significantly, and a total oocyte concentration of 2.5 mM or higher nearly eliminated GVBD (Figure 3E). These results demonstrate a dose-dependent inhibition of GVBD and suggest that Zn^{2+} inhibits Ras signaling. To investigate the site of action of Zn^{2+}, we analyzed the phosphorylation and enzymatic activity of ERK. Whereas treatment of oocytes with insulin results in robust induction of ERK phosphorylation and enzymatic activity, concurrent injection of Zn^{2+} caused a dose-dependent reduction of ERK phosphorylation and enzymatic activity that correlated with the reduction in GVBD (Figure 3F). These results suggest that Zn^{2+} inhibits signal transduction at a step upstream of ERK MAP kinase.

Discussion

CDF Proteins Positively Regulate Ras-Mediated Signaling

CDF proteins have not been reported to be involved in Ras-mediated signaling. The results presented here show that CDF proteins have an evolutionarily conserved function as positive regulators of Ras signaling. Strong loss-of-function mutations of *cdf-1* caused a partial but significant reduction of Ras signaling as evidenced by suppression of several Muv phenotypes, enhancement of a weak Vul phenotype, and defects in vulval cell fates in an otherwise wild-type background. Thus, *cdf-1* activity is necessary for full activity of the Ras pathway in *C. elegans*. Overexpression of wild-type CDF-1 enhanced Ras signaling, as indicated by enhancement of Muv phenotypes, indicating that CDF-1 is sufficient to stimulate Ras signaling in *C. elegans*.

CDF-1 is about 30% identical to vertebrate ZnT-1. Rat ZnT-1 can substitute for *C. elegans* CDF-1 in promoting vulval development, demonstrating that these proteins are functionally similar in the ability to promote Ras signaling. Overexpression of CDF-1 or ZnT-1 can potentiate meiotic maturation in *Xenopus* oocytes. Thus, CDF protein activity is sufficient to stimulate Ras signaling in vertebrate cells. These observations demonstrate that CDF proteins have a conserved function as positive modulators of Ras-mediated signaling. Furthermore, the ability of the Ras signaling pathway to respond to CDF proteins has been conserved. The finding that the Ras signaling pathway retains some function in strong loss-of-function *cdf-1* mutants indicates that *cdf-1* may be a modulator of the pathway rather than an essential component. Alternatively, *cdf-1* may have an essential function that is partially supplied by a redundant gene(s).

CDF Proteins Affect Ras Signaling by Regulating the Concentration of Zn^{2+}, and Cytosolic Zn^{2+} Negatively Regulates Ras Signaling

Vertebrate ZnT-1 was identified based on its ability to protect cells from Zn^{2+} toxicity. ZnT-1 is localized to the plasma membrane and stimulates Zn^{2+} efflux from the cytosol (Palmiter and Findley, 1995). Our results suggest that CDF-1 and ZnT-1 have a similar mechanism of action. *cdf-1(lf)* mutants are hypersensitive to zinc toxicity, demonstrating that *cdf-1* is necessary for normal zinc metabolism. *cdf-1* mutants are not hypersensitive to the toxic effects caused by cobalt, copper, or cadmium, indicating that *cdf-1* is specifically involved in zinc metabolism and that *cdf-1(lf)* mutants are not hypersensitive to nonspecific stresses. Furthermore, overexpression of CDF-1 was sufficient to prevent the Zn^{2+} inhibition of Ras-mediated signaling during vulval development. These results indicate that *cdf-1* reduces the

Table 3. Phenotype of Ras Pathway Mutants Exposed to Supplemental Zn^{2+}

Genotype	Supplemental [Zn^{2+}] (μM)[a]	Percentage Muv	N[b]
let-60(n1046gf)	0	78	338
let-60(n1046gf)	250	18	288
let-60(n1046gf); amEx28[c]	250	84	354
let-60(ga89gf)[d]	0	20	622
let-60(ga89gf)[d]	250	4	559
let-23(sa62gf)	0	82	454
let-23(sa62gf)	250	29	831
lin-15(n765)[e]	0	50	497
lin-15(n765)[e]	250	14	515
lin-1(e1275ts)[e]	0	57	534
lin-1(e1275ts)[e]	250	56	429
lin-12(n137gf)	0	98	284
lin-12(n137gf)	250	98	407

L4 hermaphrodites were placed on Petri dishes, and their progeny were scored for the Muv phenotype, one or more ventral protrusions displaced from the position of the vulva. Some of the media contained 250 μM supplemental Zn^{2+}. Unless otherwise noted, animals were raised at 20°C.

[a] Supplemental [Zn^{2+}], the final concentration of $ZnSO_4$ added to the media.

[b] N, number of hermaphrodites examined.

[c] *amEx28* is an extrachromosomal array comprised of multiple copies of pJJ4 (genomic *cdf-1*) and the transformation marker pRF4.

[d] Animals were scored at 25°C.

[e] Animals were scored at 18°C.

concentration of Zn^{2+} in an animal, since *cdf-1* function was necessary and sufficient to protect against the effects of excess supplemental zinc.

A CDF-1::GFP fusion protein was analyzed to determine the subcellular localization of CDF-1. CDF-1::GFP appeared to be localized to the plasma membrane of intestinal cells and Pn.p descendants. This is consistent with the prediction that CDF-1 is a transmembrane protein, and the same subcellular localization was demonstrated for vertebrate ZnT-1 (Palmiter and Findley, 1995). Expression of rat ZnT-1 rescued the zinc hypersensitivity of *cdf-1(lf)* mutants, demonstrating that CDF-1 and ZnT-1 are functionally interchangeable. The findings that *cdf-1* is specifically involved in Zn^{2+} metabolism and that CDF-1 is structurally and functionally similar to vertebrate ZnT-1 strongly support the model that CDF-1 functions by stimulating Zn^{2+} efflux from the cytosol.

These findings suggest that CDF proteins regulate Ras signaling by stimulating Zn^{2+} efflux; however, they do not rule out the possibility that CDF proteins affect Ras signaling by an alternative mechanism. The model that CDF proteins function by regulating the concentration of Zn^{2+} predicts that directly manipulating the concentration of Zn^{2+} will affect Ras signaling. We demonstrated that this prediction is true. The addition of supplemental zinc to worm media negatively regulated the Ras pathway, as indicated by suppression of the Muv phenotypes caused by *lin-15(lf)*, *let-23(gf)*, and *let-60(gf)*. To determine whether Zn^{2+} inhibition of Ras signaling is conserved and whether Zn^{2+} acts in the cytosol, we injected Zn^{2+} directly into the cytosol of *Xenopus* oocytes. Cytosolic Zn^{2+} inhibited Ras signaling, as indicated by suppression of meiotic maturation and ERK phosphorylation. A dose-response experiment showed that an increase in the Zn^{2+} concentration of less than 2-fold significantly reduced Ras signaling. Taken together, our results support the model that Zn^{2+} inhibits Ras-mediated signaling and that CDF proteins positively modulate the pathway by relieving Zn^{2+} inhibition. Thus, in *cdf-1(lf)* mutants, the concentration of cytosolic Zn^{2+} is elevated, and this inhibits Ras signaling; overexpression of CDF-1 or ZnT-1 lowers the concentration of cytosolic Zn^{2+} and promotes Ras signaling.

A further prediction of the model that CDF proteins regulate Ras signaling by affecting the concentration of Zn^{2+} is that CDF proteins and Zn^{2+} will act at the same position in the signaling pathway. We determined the effects of *cdf-1(lf)* mutations and supplemental Zn^{2+} on six different mutations that cause a Muv phenotype. In each case, a *cdf-1(lf)* mutation and supplemental Zn^{2+} caused a similar effect. *cdf-1(lf)* and supplemental Zn^{2+} significantly suppressed the Muv phenotypes caused by *lin-15(lf)*, *let-23(gf)* and two different *let-60(gf)* mutations. By contrast, a *cdf-1(lf)* mutation and supplemental Zn^{2+} did not suppress the Muv phenotypes caused by *lin-1(lf)* and *lin-12(gf)* mutations. These results demonstrate that CDF and Zn^{2+} act at a similar position in the Ras signaling pathway and strongly support the model that CDF proteins regulate Ras signaling by affecting the concentration of Zn^{2+}. These data can also be used to infer the position in the pathway affected by CDF proteins and Zn^{2+}. However, these epistasis experiments must be interpreted cautiously, since the Muv mutations that were used are not null alleles. In particular, Chang et al. (2000) demonstrated that vulval differentiation in *let-60(n1046gf)* mutants is partially dependent upon upstream signaling. Nevertheless, the most straightforward interpretation of these results is that *cdf-1* and Zn^{2+} function at a position in the signaling pathway that is downstream of *lin-15*, *let-23*, and *let-60* and upstream of *lin-1* and *lin-12*. The findings that the ectopic 1° vulval cell fates caused by *lin-1(lf)* and the ectopic 2° vulval cell fates caused by *lin-12(gf)* were not affected by *cdf-1(lf)* or supplemental Zn^{2+} are important because they demonstrate that increasing the concentration of Zn^{2+} does not cause a generalized cellular stress that prevents Pn.p cells from adopting vulval cell fates. The

Xenopus system was used to further investigate the position in the signaling pathway affected by CDF proteins and Zn^{2+}. Overexpression of CDF proteins, which likely caused a decrease in cytosolic Zn^{2+}, promoted the phosphorylation of ERK by MEK. Injection of Zn^{2+} into the cytosol of *Xenopus* oocytes blocked the phosphorylation and enzymatic activity of ERK. These data indicate that CDF proteins and Zn^{2+} act at the level of ERK or upstream.

The observations in *Xenopus* and *C. elegans* suggest that Zn^{2+} acts on a portion of the signaling pathway that includes the core components Ras, Raf, MEK, and ERK and modulators such as KSR. Furthermore, the protein(s) that is inhibited by Zn^{2+} and affects Ras signaling appears to be partially bound to Zn^{2+} under baseline conditions, and it binds additional Zn^{2+} when the concentration of Zn^{2+} increases. Interestingly, Raf and KSR proteins contain domains that are predicted to bind Zn^{2+}. It has been estimated that there is an extraordinary intracellular Zn^{2+} binding capacity and that free Zn^{2+} concentrations are femtomolar (Outten and O'Halloran, 2001). These observations suggest that the target(s) of Zn^{2+} that affects Ras signaling has a very high Zn^{2+} affinity, since it competes for Zn^{2+} in this intracellular environment.

The mechanism of action of CDF proteins was investigated by determining the expression pattern of CDF-1 in *C. elegans* and the site of action of CDF proteins in *C. elegans* and *Xenopus*. Injection of mRNA encoding CDF proteins into individual *Xenopus* oocytes stimulated Ras signaling, demonstrating that CDF proteins can act cell autonomously in *Xenopus* oocytes. In *C. elegans*, CDF-1 was expressed significantly in the Pn.p cell descendants and functioned cell autonomously when it was expressed in the Pn.p cells. Interestingly, CDF-1 is highly expressed in intestinal cells and can also function cell nonautonomously in the intestinal cells. These results suggest that *cdf-1* function in the intestinal cells may reduce the dietary Zn^{2+} that enters the animal and thereby reduce the concentration of Zn^{2+} in the extracellular fluid that contacts the Pn.p cells. Since there is likely to be a direct relationship between the concentration of extracellular and intracellular Zn^{2+} in the Pn.p cells, *cdf-1* function in intestinal cells may result in a lower concentration of intracellular Zn^{2+} in the Pn.p cells and enhanced Ras signaling. The finding that *cdf-1* can act cell nonautonomously in the intestinal cells is not consistent with the model that CDF functions by directly binding a protein in the Ras signaling cascade and supports the conclusion that CDF proteins regulate the Ras signaling pathway by affecting the concentration of Zn^{2+}.

Physiological Concentrations of Zn^{2+} Inhibit Ras-Mediated Signaling

The observation that increasing the concentration of Zn^{2+} inhibits Ras-mediated signaling is consistent with the model that Zn^{2+} is a physiologically significant regulator of the signaling pathway, but it is also consistent with the possibility that Zn^{2+} does not normally affect the pathway and only has an inhibitory effect when the concentration is abnormally elevated. The model that Zn^{2+} is a physiologically significant inhibitor predicts that lowering the concentration of cytosolic Zn^{2+} will enhance Ras-mediated signaling, whereas the alternative model predicts that lowering the concentration of cytosolic Zn^{2+} will not alter the Ras pathway. We investigated the effect of lowering the concentration of cytosolic Zn^{2+} by overexpressing CDF proteins. The results presented here demonstrate that overexpression of CDF-1 and ZnT-1 can stimulate Ras signaling in *Xenopus* oocytes. Furthermore, overexpression of CDF-1 in *C. elegans* stimulates Ras signaling, as evidenced by the enhancement of Muv phenotypes. These results indicate that physiological concentrations of Zn^{2+} do inhibit the Ras pathway in two different animals and, thus, that Zn^{2+} inhibition is physiologically significant and evolutionarily conserved.

The inhibition by Zn^{2+} may be a static phenomenon that reduces the baseline pathway activity and is overcome by ligand stimulation of the pathway. However, our findings raise the interesting possibility that Zn^{2+} is dynamically regulated to control the activity of the pathway, similar to the dynamic regulation of Ca^{2+}, since lowering the concentration of Zn^{2+} enhances signaling and raising the concentration of Zn^{2+} diminishes signaling. A rigorous test of this possibility will require the development of reagents that can measure Zn^{2+} concentrations in living cells.

Experimental Procedures

General Methods and Strains

C. elegans strains were cultured on NGM agar plates seeded with the *E. coli* strain OP50 and grown at 20°C unless otherwise noted (Brenner, 1974). The wild-type strain and parent of all mutant strains was N2. The following mutations that affect vulval development were used. *let-23(sa62 C359Y)* is a semidominant, gain-of-function allele that affects the extracellular domain of the LET-23 RTK (Katz et al., 1996). *lin-12(n137 S872P)* is a dominant, gain-of-function allele that affects the extracellular domain of the transmembrane LIN-12 Notch (Greenwald and Seydoux, 1990). *lin-1(e1275 R175STOP)* is a recessive, heat sensitive, partial loss-of-function allele that truncates LIN-1 downstream of the ETS DNA binding domain (Beitel et al., 1995). *lin-1(n1761)* is a gain-of-function allele caused by a single nucleotide change in the splice donor site of exon 5; the mutant LIN-1 protein is insensitive to regulation by MPK-1 MAP kinase (Jacobs et al., 1998). *let-60(n1046 G13E)* is a semi-dominant, gain-of-function allele (Beitel et al., 1990). Similar mutations of vertebrate Ras result in oncogenic proteins that have reduced GTPase activity. *let-60(ga89 L19F)* is a temperature sensitive allele that causes an increase in *let-60* activity at 25°C and a decrease in *let-60* activity at 15°C (Eisenmann and Kim, 1997). *lin-15(n765)* is a heat sensitive loss-of-function allele lacking both *lin-15A* and *lin-15B* activity; mutants have a deletion of 200 bp within the genomic region encoding the *lin-15B* transcript (Clark et al., 1994). The *cdf-1* alleles *n2527* and *ok192* are described here. The following mutations that cause a visible phenotype and were used to mark chromosomes are described by Riddle et al. (1997). LG II: *unc-4(e120)*; LG IV: *dpy-20(e1282)*; LG X: *lon-2(e678), unc-18(e81)*. We used standard methods to construct double mutants. The presence of *cdf-1(n2527)* in the *lin-1; cdf-1* and the *lin-12; cdf-1* strains was confirmed by DNA sequencing.

The identification of the *n2527* mutation was described previously (Jakubowski and Kornfeld, 1999). The *ok192* deletion allele was identified by the *C. elegans* gene knockout consortium by PCR screening mutagenized worms using oligonucleotide primers that amplified 2.9 kb beginning 50 bp upstream of exon 1 and ending 532 bp into exon 4. We determined the deletion boundaries by sequencing genomic DNA that was PCR amplified from *ok192* worms.

Identification and Analysis of *cdf-1* cDNAs

Unless otherwise noted, molecular biology techniques were performed as described by Sambrook et al. (1989). We used two cDNA libraries that were generated with RNA derived from mixed stage populations of *C. elegans* (Kohn et al., 2000). Approximately 180,000 bacteriophage plaques were hybridized with a mixture of three radiolabeled PCR products that were amplified from genomic DNA and spanned exons 2–7 of predicted open reading frame C15B12.7. Three hybridizing bacteriophages were isolated. The cDNA yk14a5 was obtained from the *C. elegans* EST project (Kohara, 1996).

The complete DNA sequence of all four cDNA clones was determined. The positions of *cdf-1* exons on cosmid C15B12, which was sequenced (*C. elegans* Sequencing Consortium, 1998), are as follows: exon 1, 41,666–41,487; exon 2, 39,892–39,804; exon 3, 39,751–39,589; exon 4, 39,189–38,538; exon 5, 38,458–38,297; exon 6, 37,806–37,503; exon 7, 37,452–36,991. At its 5′ end, *cdf-1* cDNA #1 contained four nucleotides of the SL1 *trans*-spliced leader sequence fused to *cdf-1* at 41,666 (exon 1) and it extended to 37,297 (exon 7) at its 3′ end. *cdf-1* cDNA #2 extended from 40,065 (intron 1) to 37,298 (exon 7). *cdf-1* cDNA #3 extended from 38,826 (exon 4) to 36,991 (exon 7). *cdf-1* cDNA yk14a5 extended from 39,090 (exon 4) to 36,991 (exon 7), at which point it contained at least 25 consecutive deoxyadenine residues indicative of the poly(A) tail.

DNA Cloning

The plasmid pJJ4, which we previously described, consists of pBluescript (Stratagene) containing a 6239 bp fragment of genomic DNA that extends from 1612 bp upstream of the predicted *cdf-1* START codon to 384 bp downstream of the predicted STOP codon (Jakubowski and Kornfeld, 1999). To generate pJJ16, we inserted an 867 bp DNA fragment containing coding sequence for GFP interrupted by three introns at the position of the *cdf-1* STOP codon. GFP was derived from the plasmid pPD95.77 (Chalfie et al., 1994). pJJ16 encodes a CDF-1::GFP fusion protein. To generate pJJ17, we modified pJJ16 by replacing the genomic DNA encoding *cdf-1* with a full-length 1.5 kb *cdf-1* cDNA. pJJ17 encodes a CDF-1::GFP fusion protein. To generate pJJ23, we modified pJJ16 by replacing the genomic DNA encoding *cdf-1* with a full-length 1.9 kb rat *ZnT-1* cDNA (Palmiter and Findley, 1995). pJJ23 encodes a ZnT-1::GFP fusion protein. To generate pJJ24, we inserted a full-length 1.5 kb *cdf-1* cDNA fused to DNA encoding GFP (derived from pJJ17) into the *ges-1* promoter-containing plasmid pJM16 (Aamodt et al., 1991). pJJ24 encodes a CDF-1::GFP fusion protein that is predicted to be expressed only in the intestinal lineage. To generate pJJ25, we inserted a full-length 1.5 kb *cdf-1* cDNA fused to DNA encoding GFP (derived from pJJ17) into the *lin-31* promoter-containing plasmid pB255 (Tan et al., 1998). pJJ25 encodes a CDF-1::GFP fusion protein that is predicted to be expressed predominantly in the vulval precursor cells.

Transgenic Strain Construction

Transgenic worm strains were generated by germline transformation as described by Mello et al. (1991). We coinjected worms with pJJ4, pJJ16, pJJ17, pJJ23, pJJ24, or pJJ25 (10 ng/μl) and plasmid pRF4 (90 ng/μl), which contains the dominant mutation *rol-6(su1006)*. We established an independently derived transgenic strain from each F1 animal that displayed the Rol phenotype and segregated F2 progeny that displayed the Rol phenotype.

Heavy Metal Ion Sensitivity Assays

Molten NGM agar was supplemented with a solution of $ZnSO_4$, $CoCl_2$, $CdCl_2$, or $CuSO_4$, dispensed in Petri dishes, and seeded with *E. coli* OP50 (which grew normally). Development was analyzed by placing L4 hermaphrodites on metal-supplemented plates, transferring adults to fresh metal-supplemented plates after one day and allowing the adults to deposit eggs for 3 hr. Eggs were picked to separate metal-supplemented plates and monitored daily. Larval stages were assessed by the size and morphology of animals and the presence of shed cuticles. The adult stage was assessed by the size of animals and the presence of a vulva and/or eggs. Adults were classified as fertile if they generated embryos that hatched.

Xenopus Oocyte Microinjection and Protein Analysis

cDNAs encoding *cdf-1* and rat *Znt-1* were subcloned into plasmid pXen1 (MacNicol et al., 1997). The plasmid pSP64T-Ha-Ras^{V12} encodes constitutively active Ha-Ras. To prepare mRNA for *Xenopus* oocyte expression, we linearized plasmids and produced mRNA using the SP6 mMESSAGE mMACHINE in vitro transcription kit (Ambion). RNA production was verified by agarose gel electrophoresis.

Oocytes were surgically removed from mature females and defolliculated by incubation in 1 mg/ml of collagenase (Sigma type I) for 3–4 hr. Fully grown stage VI oocytes were allowed to recover at 19°C in medium containing 88 mM NaCl, 1 mM KCl, 2.4 mM $NaHCO_3$, 0.82 mM $MgSO_4$, 10 mM HEPES (pH 7.4), 0.33 mM $Ca(NO_3)_2 \cdot 4H_2O$, 0.41 mM $CaCl_2 \cdot 2H_2O$, 1 g/l BSA, 1 g/l Ficoll 400, and 10 μg/ml of penicillin-streptomycin. Within 18 hr of isolation, oocytes were injected with water or 50 ng of either *cdf-1* or *Znt-1* RNA; 12–24 hr later, the oocytes were reinjected with 15 ng of *Ha-Ras*^{V12} RNA or stimulated with 7.5 μM bovine pancreas insulin (Sigma). Insulin stimulation was carried out in modified OR-2 medium containing 83 mM NaCl, 0.5 mM $CaCl_2$, 1 mM $MgCl_2$, and 10 mM HEPES (pH 7.8) (Maller and Koontz, 1981). At various times following the addition of insulin or *Ha-Ras*^{V12} injection, oocytes were scored for the presence of a broad white spot on the animal pole, an indication of GVBD.

To analyze the effect of Zn^{2+}, we prepared oocytes as described above and injected 15 nl of a $ZnSO_4$ solution of varying concentrations within 18 hr of oocyte isolation. Oocytes were incubated for 12 hr at 19°C, stimulated with 7.5 μM insulin for 24 hr, and assessed for GVBD. We calculated the total oocyte Zn^{2+} concentration using the following equation:

$$[Zn^{2+}]_{total} = \frac{([Zn^{2+}]_{oocyte})(Volume_{oocyte}) + ([Zn^{2+}]_{injected})(Volume_{injected})}{Volume_{oocyte} + Volume_{injected}}$$

To prepare Western blots, we lysed oocytes using NP40 lysis buffer, prepared a protein extract, resolved the proteins by SDS-PAGE, and electrophoretically transferred the proteins to nitrocellulose membranes. The membranes were blocked with 5% nonfat dry milk in TBST and incubated overnight at 4°C with rabbit polyclonal anti-ERK antibody (Santa Cruz Biotech) or rabbit polyclonal anti-phospho-ERK antibody (New England Biolabs Inc.). Bound antibody was visualized using an alkaline phosphatase-conjugated secondary antibody and the appropriate color-developing agents.

ERK MAP kinase assays were performed using a kit from Cell Signaling according to the manufacturer's instructions. In brief, anti-phospho-ERK immunoprecipitates derived from oocyte cytosolic lysates were mixed with recombinant substrate protein Elk-1, 200 mM ATP, and kinase reaction buffer. Kinase reactions were terminated after a 30 min incubation period, and proteins were separated by SDS-PAGE and analyzed by immunoblotting with a specific anti-phospho-Elk-1 antibody.

Acknowledgments

We thank Andreas Szabados and Janet O'Neal for assistance with genetic analysis, Gary Molder and Bob Barstead for providing cDNA libraries and the *cdf-1(ok192)* allele, Yuji Kohara for providing cDNA, Deborah Morrison, Richard Palmiter, Stuart Kim, Jim McGhee, and Andy Fire for providing plasmids, and Tim Schedl, Stuart Kornfeld, and members of the K. Kornfeld lab for advice about the manuscript. Some strains were provided by the *Caenorhabditis elegans* Genetics Center (St. Paul, MN), which is funded by the National Center for Research Resources of the National Institutes of Health. This research was supported by grants from the NIH to A.J.M (GM54670) and K.K. (CA84271) and the Monsanto-Pharmacia/Washington University Biomedical Program (A.J.M. and K.K.). A.J.M. is an established investigator of the American Heart Association. K.K. is a recipient of a Burroughs Wellcome Fund New Investigator Award in the Basic Pharmacological Sciences and a Scholar Award from the Leukemia and Lymphoma Society.

Received: September 6, 2001
Revised: March 18, 2002

References

Aamodt, E.J., Chung, M.A., and McGhee, J.D. (1991). Spatial control of gut-specific gene expression during *Caenorhabditis elegans* development. Science *252*, 579–582.

Barbacid, M. (1987). *ras* genes. Annu. Rev. Biochem. *56*, 779–827.

Beitel, G.J., Clark, S.G., and Horvitz, H.R. (1990). *Caenorhabditis elegans ras* gene *let-60* acts as a switch in the pathway of vulval induction. Nature *348*, 503–509.

Beitel, G.J., Tuck, S., Greenwald, I., and Horvitz, H.R. (1995). The *Caenorhabditis elegans* gene *lin-1* encodes an ETS-domain protein and defines a branch of the vulval induction pathway. Genes Dev. *9*, 3149–3162.

Brenner, S. (1974). The genetics of *Caenorhabditis elegans.* Genetics *77*, 71–94.

C. elegans Sequencing Consortium (1998). Genome sequence of the nematode *C. elegans*: a platform for investigating biology. Science *282*, 2012–2018.

Cantley, L.C., Auger, K.R., Carpenter, C., Duckworth, B., Graziani, A., Kapeller, R., and Soltoff, S. (1991). Oncogenes and signal transduction. Cell *64*, 281–302.

Chalfie, M., Tu, Y., Euskirchen, G., Ward, W.W., and Prasher, D.C. (1994). Green fluorescent protein as a marker for gene expression. Science *263*, 802–805.

Chang, C., Hopper, H.A., and Sternberg, P.W. (2000). *Caenorhabditis elegans* SOS-1 is necessary for multiple RAS-mediated developmental signals. EMBO J. *19*, 3283–3294.

Clark, S.G., Lu, X., and Horvitz, H.R. (1994). The *Caenorhabditis elegans* locus *lin-15*, a negative regulator of a tyrosine kinase signaling pathway, encodes two different proteins. Genetics *137*, 987–997.

Conklin, D.S., McMaster, J.A., Culbertson, M.R., and Kung, C. (1992). *COT1*, a gene involved in cobalt accumulation in *Saccharomyces cerevisiae.* Mol. Cell. Biol. *12*, 3678–3688.

Dickson, B., and Hafen, E. (1994). Genetics of signal transduction in invertebrates. Curr. Opin. Genet. Dev. *4*, 64–70.

Eisenmann, D.M., and Kim, S.K. (1997). Mechanism of activation of the *Caenorhabditis elegans ras* homologue *let-60* by a novel, temperature-sensitive, gain-of-function mutation. Genetics *146*, 553–565.

Greenwald, I. (1997). Development of the vulva. In *C. elegans* II, D.L. Riddle, T. Blumenthal, B.J. Meyer, and J.R. Priess, eds. (Cold Spring Harbor, New York: Cold Spring Harbor Laboratory Press), pp. 519–541.

Greenwald, I., and Seydoux, G. (1990). Analysis of gain-of-function mutations of the *lin-12* gene of *Caenorhabditis elegans.* Nature *346*, 197–199.

Horvitz, H.R., and Sternberg, P.W. (1991). Multiple intercellular signalling systems control the development of the *Caenorhabditis elegans* vulva. Nature *351*, 535–541.

Huang, L.S., Tzou, P., and Sternberg, P.W. (1994). The *lin-15* locus encodes two negative regulators of *Caenorhabditis elegans* vulval development. Mol. Biol. Cell *5*, 395–412.

Jacobs, D., Beitel, G.J., Clark, S.G., Horvitz, H.R., and Kornfeld, K. (1998). Gain-of-function mutations in the *Caenorhabditis elegans lin-1* ETS gene identify a C-terminal regulatory domain phosphorylated by ERK MAP kinase. Genetics *149*, 1809–1822.

Jakubowski, J., and Kornfeld, K. (1999). A local, high-density, single-nucleotide polymorphism map used to clone *Caenorhabditis elegans cdf-1.* Genetics *153*, 743–752.

Kamizono, A., Nishizawa, M., Teranishi, Y., Murata, K., and Kimura, A. (1989). Identification of a gene conferring resistance to zinc and cadmium ions in the yeast *Saccharomyces cerevisiae.* Mol. Gen. Genet. *219*, 161–167.

Katz, W.S., Lesa, G.M., Yannoukakos, D., Clandinin, T.R., Schlessinger, J., and Sternberg, P.W. (1996). A point mutation in the extracellular domain activates LET-23, the *Caenorhabditis elegans* epidermal growth factor receptor homolog. Mol. Cell. Biol. *16*, 529–537.

Kohara, Y. (1996). Large scale analysis of *C. elegans* cDNA. Tanpakushitsu Kakusan Koso *41*, 715–720.

Kohn, R.E., Duerr, J.S., McManus, J.R., Duke, A., Rakow, T.L., Maruyama, H., Moulder, G., Maruyama, I.N., Barstead, R.J., and Rand, J.B. (2000). Expression of multiple UNC-13 proteins in the *Caenorhabditis elegans* nervous system. Mol. Biol. Cell *11*, 3441–3452.

Korn, L.J., Seibu, C.W., McCormick, F., and Roth, R.A. (1987). Ras p21 as a potential mediator of insulin action in *Xenopus* oocytes. Science *236*, 840–843.

Kornfeld, K. (1997). Vulval development in *Caenorhabditis elegans.* Trends Genet. *13*, 55–61.

Kornfeld, K., Guan, K.L., and Horvitz, H.R. (1995a). The *Caenorhabditis elegans* gene *mek-2* is required for vulval induction and encodes a protein similar to the protein kinase MEK. Genes Dev. *9*, 756–768.

Kornfeld, K., Hom, D.B., and Horvitz, H.R. (1995b). The *ksr-1* gene encodes a novel protein kinase involved in Ras-mediated signaling in C. elegans. Cell *83*, 903–913.

Lackner, M.R., Kornfeld, K., Miller, L.M., Horvitz, H.R., and Kim, S.K. (1994). A MAP kinase homolog, *mpk-1*, is involved in *ras*-mediated induction of vulval cell fates in *Caenorhabditis elegans.* Genes Dev. *8*, 160–173.

MacNicol, M.C., Pot, D., and MacNicol, A.M. (1997). pXen, a utility vector for the expression of GST-fusion proteins in *Xenopus laevis* oocytes and embryos. Gene *196*, 25–29.

Maller, J.L., and Koontz, J.W. (1981). A study of the induction of cell division in amphibian oocytes by insulin. Dev. Biol. *85*, 309–316.

Marshall, C.J. (1994). MAP kinase kinase kinase, MAP kinase kinase and MAP kinase. Curr. Opin. Genet. Dev. *4*, 82–89.

McMahon, R.J., and Cousins, R.J. (1998). Mammalian zinc transporters. J. Nutr. *128*, 667–670.

Mello, C.C., Kramer, J.M., Stinchcomb, D., and Ambros, V. (1991). Efficient gene transfer in *C. elegans*: extrachromosomal maintenance and integration of transforming sequences. EMBO J. *10*, 3959–3970.

Nomizu, T., Falchuk, K.H., and Vallee, B.L. (1993). Zinc, iron, and copper contents of *Xenopus laevis* oocytes and embryos. Mol. Reprod. Dev. *36*, 419–423.

Outten, C.E., and O'Halloran, T.V. (2001). Femtomolar sensitivity of metalloregulatory proteins controlling zinc homeostasis. Science *292*, 2488–2492.

Palmiter, R.D., and Findley, S.D. (1995). Cloning and functional characterization of a mammalian zinc transporter that confers resistance to zinc. EMBO J. *14*, 639–649.

Palmiter, R.D., Cole, T.B., and Findley, S.D. (1996). ZnT-2, a mammalian protein that confers resistance to zinc by facilitating vesicular sequestration. EMBO J. *15*, 1784–1791.

Paulsen, I.T., and Saier, M.H., Jr. (1997). A novel family of ubiquitous heavy metal ion transport proteins. J. Membr. Biol. *156*, 99–103.

Riddle, D.L., Blumenthal, T., Meyer, B.J., and Priess, J.R., eds. (1997). *C. elegans* II (Cold Spring Harbor, New York: Cold Spring Harbor Laboratory Press).

Sambrook, J., Fritsch, E.F., and Maniatis, T. (1989). Molecular Cloning: A Laboratory Manual, Second Edition (Cold Spring Harbor, New York: Cold Spring Harbor Laboratory Press).

Sternberg, P.W., and Han, M. (1998). Genetics of RAS signaling in *C. elegans.* Trends Genet. *14*, 466–472.

Tan, P.B., Lackner, M.R., and Kim, S.K. (1998). MAP kinase signaling specificity mediated by the LIN-1 Ets/LIN-31 WH transcription factor complex during *C. elegans* vulval induction. Cell *93*, 569–580.

Xing, H., Kornfeld, K., and Muslin, A.J. (1997). The protein kinase KSR interacts with 14-3-3 protein and Raf. Curr. Biol. *7*, 294–300.